Proceedings of the 2004 IEEE
International Conference on Robotics & Automation
New Orleans, LA • April 2004

Mass/ Inertia and Joint Friction Minimization for a Low–force Five–dof Haptic Device *

Kostas Vlachos and Evangelos Papadopoulos
Department of Mechanical Engineering
National Technical University of Athens
15780 Athens, Greece
{kostaswl, egpapado}@central.ntua.gr

Dionissios N. Mitropoulos
School of Medicine
National Kapodistrian University of Athens
11527 Athens, Greece
dmp@otenet.gr

***Abstract*— This paper presents a design methodology, which aims at the minimization of the mass, inertia and joint friction for a low – force five – dof haptic device. The haptic device is optimized along a typical path with proper tolerances, rather than at some workspace operating point. The device, part of a training medical simulator for urological operations, consists of a two dof, 5–bar linkage and a three dof spherical joint. The requirement for reliable reproduction of low torques and forces lead to the need for minimization of device induced parasitic forces and torques. The multiobjective optimization employed is based on two objective functions that include mass/ inertia properties and joint friction. Kinematical and operational constraints are taken into account. The resulting optimized mechanism is substantially improved with respect to an existing device.**

Keywords*— Force feedback, multiobjective optimization, haptic devices, training medical simulators

I. Introduction

The use of simulators is now an accepted tool in the training of surgeons, [1]. Although it is still early for definitive conclusions, it seems that there are many advantages in the use of simulators. Simulator-based training is less expensive and results in efficient and customizable training in complex operations, [2]. Training on patients can result in serious damages and lawsuits while training on animals becomes an undesirable alternative for ethical and economical reasons. Furthermore the anatomy of an animal is not always close enough to that of the human. Also, the existence of a training simulator increases the availability of the training environment, allows an easier evaluation of the performance of the trainee, and can be used to introduce various operation scenarios or situations.

Realistic medical simulators consist of a graphical environment, which reproduces the visual information that the surgeon obtains during an operation, and a haptic device, which reproduces the haptic information. Today, one can distinguish two trends in the development of medical simulators. The first is characterized by the use of general-purpose haptic devices, like the Phantom or the Freedom – 7, [3, 4, 5]. The second trend is characterized by the use of haptic devices designed for a specific operation, [6, 7, 8, 9].

The faithful reproduction of the real forces and torques that the surgeon feels during an operation is of great importance. This means that the mechanism should be transparent as much as possible. Optimization techniques have been already used in improving the performance of mechanisms and manipulators.

The inertial and acceleration characteristics of manipulators have been discussed in [10]. Optimization techniques are used to determine the smallest inertial properties and the maximum achievable acceleration of the end-effector in every direction over the workspace. A global isotropy index has been proposed to quantify a configuration independent isotropy of a robot's Jacobian or mass matrix, [11]. This index was used to compare the performance of three manipulators, including two parallel platform robots and a hybrid robot, [12]. A two degree-of-freedom (dof) haptic device was optimized with respect to workspace, intrusion, inertia, response and structural properties, [13]. The architecture of a parallel redundant mechanism has been optimized from a kinematic viewpoint, [14]. The dexterity, uniformity and actuator forces have been investigated as potential objective functions. Authors' previous work has presented the design of a five dof haptic interface, which was partly optimized with respect to its condition number and perceived inertia under several kinematic constraints, [9].

This paper presents a multiobjective optimization methodology resulting in an improved low–force five–bar haptic device, which is a part of a training medical simulator for urological operations. Unlike other haptic devices in which the reproduction of large forces or torques is of prime importance, here it is desired to build a device that can reproduce faithfully very small forces and torques, such as those appearing in urological operations. To this end, a major effort is placed in designing the mechanism such that it is characterized by low mass and inertia and small joint friction. Two objective functions are defined, the first focusing at mass/ inertia optimization and the second at joint friction. The optimal design is achieved for a typical endoscope path, allowing at the same time small deviations from it. The methodology results in an optimum mechanism geometry and an optimum location of the endoscope path with respect to the haptic device base. The proposed optimization methodology is suitable for any mechanism that should be optimized along a given path. The paper describes in detail the objective functions employed, the optimization constraints and the

* Support of this work by the PENED and PRAXE programs of the Hellenic General Secretariat for Research and Technology is acknowledged.

overall procedure. Finally, optimization results are presented and discussed.

II. Description of the Haptic Device

As mentioned above, the haptic device is used in a training simulator for urological operations. During a urological operation on a male patient, the surgeon inserts a long cylindrical endoscope until its endpoint reaches the patient's bladder. During insertion, the endoscope follows a path such as the typical one shown in Fig. 1. The surgeon moves the tip of the endoscope from the insertion point A to the final point C, via an intermediate point B, see Fig. 1. At point B, the endoscope orientation changes without translation, so as to align the entire urethra and continue the insertion phase without traumas. The corresponding endoscope configurations labeled by a, b, c, d, are shown in Fig. 1.

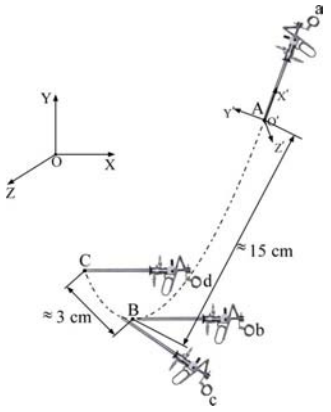

Figure 1. The Path

When the tip of the endoscope reaches the bladder (point C in Fig. 1), the surgeon inserts through the endoscope a mechanism with a scissor-like handle and begins the second phase. This phase is the main operation in which tissue removal occurs. During this phase, the movements of the endoscope are mainly rotational. The actual kinematic requirements that define the minimum workspace of the haptic interface are shown in Table I. These were found by actual observations of typical urological operations.

TABLE I. Haptic Device Workspace Requirements

Motion	Lengths
Translation along the X axis	0.1 m
Translation along the Y axis	0.1 m
Translation along the Z axis	0.0 m
Rotation about the X' axis	±180°
Rotation about the Y' axis	±30°
Rotation about the Z' axis	±30°

Observations during our previous work showed that a haptic mechanism with two translational and three rotational dof is needed, [9]. The mechanism, shown in Fig. 2, consists of a two dof, 5–bar linkage and a three dof spherical joint. To reduce mechanism moving mass and inertia, all actuators are placed at the base. The transmission system is implemented using tendon drives with capstans, [9].

The forces that the surgeon feels during the operation are small but of great importance, because they provide the necessary feedback for the successful accomplishment of the operation. In order to reproduce these small forces, the haptic mechanism must have low mass and inertia, low friction, no backlash, and be absolutely backdriveable, [9]. The upper limits of forces and torques during a urological operation were measured in collaboration with specialist surgeons and are shown in Table II. However, the minimum forces and torques that are actually felt during an operation can be a fraction of these limits.

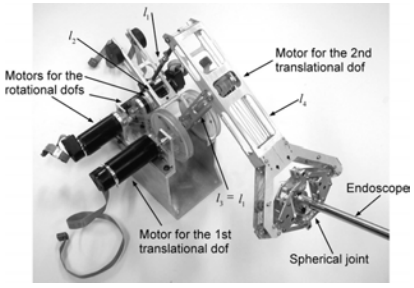

Figure 2. The first version of the haptic device

TABLE II. Force/torque Upper Limits During an Operation

Motion	Lengths
Force along the X axis	4.50 N
Force along the Y axis	4.50 N
Torque about the X' axis	10.00 mNm
Torque about the Y' axis	150.00 mNm
Torque about the Z' axis	150.00 mNm

In the first version of the haptic device, see Fig. 2, the link lengths of the five – bar mechanism were optimized in order to minimize the condition number of the mechanism along a path, under kinematical and structural constraints. The path was fixed in space relative to the mechanism base. Table III presents the optimized configuration.

TABLE III. Previous Work Results

Link	Length
$l_1 = l_3$	0.135 m
l_2	0.075 m
l_3	0.135 m
l_4	0.23 m

III. Optimization Design

The problem that we present here is more complex. All the link lengths are free to be optimized. The path that the mechanism should follow is free in space relative to the base. The optimization results are these unknown parameters under several kinematical and implementation constraints.

The schematic view of the 2 – dof 5 – bar mechanism, which is going to be optimized, and of a typical path, in a random location, to follow is illustrated in Fig. 3. The symbols are explained in Table IV.

TABLE IV. SYMBOL EXPLANATION OF FIGURE 3

Symbol	Explanation
$l_1 = l_3$	Length of link 1
l_2	Length of link 2
l_3	Length of link 3
l_4	Length of link 4
l_{4-2}	Length of link 4 – Length of link 2
q_1	Angle between link 1 and X axis
q_2	Angle between link 2 and X axis

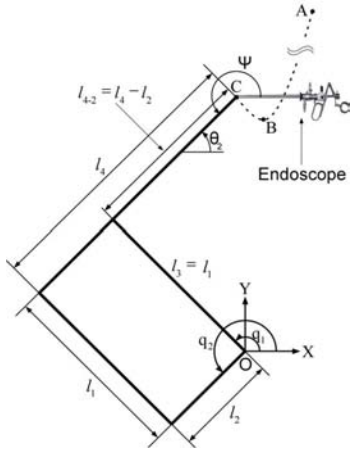

Figure 3. Schematic view of the 5-bar linkage and of a random located typical path to follow.

The optimization goal is to find the mechanism link lengths and the location of the path ABC with respect to the base point O, so that mass, inertia and friction at the joints of the 5 – bar mechanism are minimized. Because of the nature of the surgical operation, the path ABC lies always on the XY plane. Also, because the patient assumes a constant and predetermined position with respect to the vertical, the same applies to the orientation of path ABC. Because of these observations, the relative location of path ABC with respect to the haptic interface base point O can be described by two parameters that locate one of its point with respect to O.

Next, two objective functions f_1, and f_2 are defined that can be used as the objective function f in a multiobjective optimization approach.

A. The first minimization

1) The first objective function f_1

The diagonal terms of the mass matrix of the 5 – bar mechanism depend on the length, the mass and the inertia of the links. We assume that the links are cylinders with mass

$$m(l) = \rho \frac{\pi}{4}\left(b^2 - a^2\right) l \tag{1}$$

where ρ is the density, b is the outer diameter, a is the inner diameter and l is the length of the link. The link inertia is

$$I(l) = m(l)\left(3a^2 + 3b^2 + l^2\right)/12 \tag{2}$$

Mass and inertia are functions of link lengths. Hence, the first objective function can be the sum of the link lengths. The minimization of this sum results in the minimization of mechanism mass and inertia.

$$f_1 = l_1 + l_2 + l_3 + l_{4-2} \tag{3}$$

A more exact optimization of the mechanism mass and inertia properties would require the minimization of the mass matrix as seen from the endoscope side, $\tilde{\mathbf{M}}$, [9], but this would make the procedure too complicated. Instead we chose the above function, Eq. (3), which is very simple and results in an optimum with a very good approximation.

In addition to the above objective, one has to take into account several conflicting kinematical and implementation constraints.

2) Constraints for the first objective function

An important constraint is that the mechanism must be large enough to follow typical endoscope paths, such as the one shown in Fig. 1. The following inequality pair describes this constraint for all points along the path,

$$\left(l_3 - l_{4-2}\right) \le \sqrt{x(s)^2 + y(s)^2} \le \left(l_3 + l_{4-2}\right) \tag{4}$$

where $x(s), y(s)$ are the coordinates of the mechanism tip along the path.

The mechanism should be well conditioned at all configurations. It can be shown that the mechanism condition number is optimum when $l_{4-2} \equiv l_4 - l_2 = l_1 \equiv l_3$ and $q_2 - q_1 = \pi/2$, while it increases when $l_{4-2} \neq l_1$ and $q_2 - q_1 \neq \pi/2$. The above gives us the following constraint,

$$1 - e_1 \le \frac{l_3}{l_{4-2}} \le 1 + e_1 \tag{5}$$

$$\frac{\pi}{2} - e_2 \le q_2 - q_1 \le \frac{\pi}{2} + e_2 \tag{6}$$

where e_1, e_2 indicates how strictly the constraint is.

It is important that Eq. (6) holds more strictly at the end position of the path, point C in Fig.1, where the main operation takes place. This introduces the next constraint,

$$\frac{\pi}{2} - e_3 \le q_{2,C} - q_{1,C} \le \frac{\pi}{2} + e_3 \tag{7}$$

where $e_2 > e_3$ and the subscript in $q_{i,C}, i = 1, 2$ denotes the values of angles q_i at point C.

Another requirement result from implementation constraints, i.e. to avoid collision between link 4 and the endoscope, the angle $\Psi = q_2$ that is formed by link 4 and the endoscope, see Fig. 3, has to be bounded according to

$$1.22rad \le q_2 \le 5.41rad \quad (8)$$

which forms another optimization constraint.

It is possible, during the training procedure, that the simulator trainees make mistakes, i.e. they may deviate from the ideal path. In this case, the haptic device must have the capability not only to follow these wrong paths, but also to maintain an optimum functionality. In collaboration with specialists we determined that the possible erroneous distance is about $e = 0.01m$ from the typical path.

Therefore, it is important to locate not path ABC with respect to O but a whole family of paths that lie within the bounds defined by the possible deviation e. In other words we find not the optimum location of the typical path, but the optimum location of an area about the typical path. This requirement leads to additional constraints.

The mechanism has to follow the perturbed paths,

$$\left(l_3 - l_{4-2}\right) \le \sqrt{x_-(s)^2 + y_-(s)^2} \le \left(l_3 + l_{4-2}\right) \quad (9)$$

$$\left(l_3 - l_{4-2}\right) \le \sqrt{x_+(s)^2 + y_+(s)^2} \le \left(l_3 + l_{4-2}\right) \quad (10)$$

where the subscript in $x_-(s), y_-(s)$ and $x_+(s), y_+(s)$ denotes the minimum and maximum perturbation about the ideal path respectively.

The mechanism should be well conditioned even in the perturbed path,

$$\begin{aligned} \frac{\pi}{2} - e_4 \le q_{2+} - q_{1+} \le \frac{\pi}{2} + e_4 \\ \frac{\pi}{2} - e_5 \le q_{2-} - q_{1-} \le \frac{\pi}{2} + e_5 \end{aligned} \quad (11)$$

where the subscript in $q_{i,+}, i = 1, 2$ and $q_{i,-}, i = 1, 2$ denotes the values of the angles at the maximum and minimum wrong locations respectively.

Finally the last optimization constraints for the perturbed paths is due to the same implementation constraints as in Eq. (8)

$$\begin{aligned} 1.0rad \le q_{2+} \le 5.585rad \\ 1.0rad \le q_{2-} \le 5.585rad \end{aligned} \quad (12)$$

Equations (4) to (12) form the set of optimization constraints for the first objective function.

If we look carefully at the objective function and the optimization constraints, we see that the length of link 2 (l_2) is not affected by the various constraints. This means that the optimization procedure will always yield as optimum length of link 2 the predefined lower bound.

Assuming a small l_2, then mass and inertia is reduced. However to transmit given forces or torques, the internal forces at the joint of the mechanism increase resulting in a high level of friction in the mechanism. This effect is made worse given the fact that the mechanism includes tendon drives, which have some non-zero preload. On the other hand, if l_2 is made large, then friction is reduced, but the inertia and mass due to l_2 is increased. These observations introduce the second minimization.

B. The second minimization

1) The second objective function f_2

We wish to minimize the friction that appears at the joints of the 5 – bar mechanism. The friction is directly proportional to the internal constraint forces at the joints according to the relation $M = Rr$, see Fig. 4, where r is the radius of the joint axle and R represents the friction force at the joint. In order to find these forces we construct the free – body diagram of each link of the mechanism.

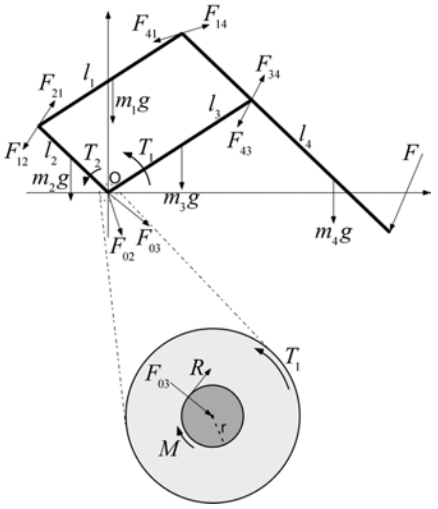

Figure 4. Mechanism internal forces and actuator torques.

The actuator forces and torques are shown in Fig.4. F is an external force, F_{ij} is the constraint force from link i to link j, T_1, T_2 are the applied torques by the actuators to links, to keep the mechanism in balance against F, m_i is the mass of link i and g is the gravitational acceleration. For each link force and moment balance equations must hold, i.e.

$$\sum F_{ij} = 0 \quad (13a)$$

$$\sum M_{Gij} = 0 \quad (13b)$$

The lower part of Fig. 4 shows a magnification of the axle and bearing including the actuated forces and torques at the base of the 5 – bar mechanism where link 3 is coupled with the corresponding actuator. T_1 is the torque, from the actuator to the link, F_{03} is the constraint force from the base to link 3, r is the radius of the axle, R represents the friction force at the joint and M is the friction that appears.

Equations (13) lead to a set of twelve equations with twelve unknowns. Solving this set yields the mechanism constraint forces and the actuator torques. Fig. 5 shows the solution of the set as function of l_2 at a specific point, namely the end of the path, or point C in Fig. 1. We see that the internal forces decrease as length l_2 increases. In the same figure, one can also observe that a minimum exists for the sum of the torques T_1, T_2. This is due to the fact that as l_2 decreases, the internal forces and therefore the friction at the joints increases. This also

increases the torques needed to compensate for friction. Therefore the sum of the torques would be a suitable objective function to minimize.

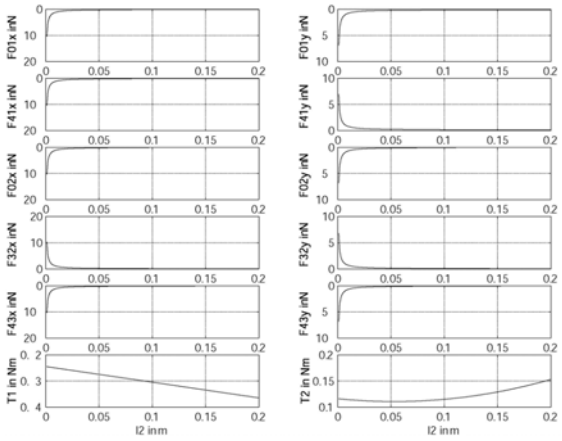

Figure 5. Constraint forces and torques at the end of the path (point C) as l_2 increases from 0.001m to 0.2m.

It is also desirable to find the optimum length not for a specific configuration but along the whole path. Therefore we divide the path in n segments. $\mathbf{T}_1, \mathbf{T}_2$ are vectors with the actuator torques at the n segments of the path.

$$\mathbf{T}_i = [T_{i,1}(s_1), ..., T_{i,n}(s_n)]' \tag{14}$$

where, $i = 1, 2$.

We define the second objective function as the sum of the infinity norms of the vectors $\mathbf{T}_1, \mathbf{T}_2$.

$$f_2 = w_1 Norm(\mathbf{T}_1, \inf) + w_2 Norm(\mathbf{T}_2, \inf) \tag{15}$$

where,

$$Norm(\mathbf{T}_i, \inf) = \max(\left(T_{i,k}\left(s_k\right)\right)() \tag{16}$$

and w_1, w_2 are the appropriate weights in order to weigh the contribution of the two actuators equally. $k = 1, ..., n$.

2) Constraints for the second objective function

The first constraint is due to implementation limitations, i.e. l_2 must have a minimum length,

$$l_2 \geq 0.06m \tag{17}$$

Next, we wish to bound the internal constraint forces at the joints of the mechanism to a acceptable limit. We construct vectors $\mathbf{F}_i$ with the internal constraint forces F_i at the n segments of the path,

$$\mathbf{F}_i = [F_{i,1}(s_1), ..., F_{i,n}(s_n)]' \tag{18}$$

where, $i = 1, ..., 12$ and then we construct matrix $\mathbf{F}$, which contains the $\mathbf{F}_i$. The second optimization constraint is the following,

$$Norm(\mathbf{F}, \inf) \leq g \tag{19}$$

where, g represents the maximum predefined acceptable friction limit.

IV. Optimization Results

For the optimization we used the Matlab optimization toolbox and the function "fgoalattain". This function is based on a Sequential Quadratic Programming (SQP) method with a few modifications, [15]. The function solves the goal attainment problem, which is one formulation for minimizing a multiobjective optimization problem. The starting guess is given in Table V. The lower and upper bounds are shown in Table VI.

TABLE V. Starting Guess at the Solution

Optimized variables	Starting Guess
Link 1, l_1	0.01 m
Link 2, l_2	0.01 m
Link 3, l_3	0.01 m
Link 4, l_4	0.02 m
X position of point C	0.0 m
Y position of point C	0.0 m

TABLE VI. Lower and Upper Bounds

Optimized variables	Lower bounds	Upper bounds
Link 1, l_1	0.01 m	0.15 m
Link 2, l_2	0.01 m	0.15 m
Link 3, l_3	0.01 m	0.15 m
Link 4, l_4	0.02 m	0.30 m
X position of point C	-0.50 m	0.50 m
Y position of point C	-0.50 m	0.50 m

The function "fgoalattain" may only give local solutions. Therefore the optimization search area is divided in several subspaces. The best result of all is chosen as the optimum.

The optimal results are shown in Tables VII and VIII and graphically in Fig.6, where the subscript in $q_{i,s}, i = 1, 2$ and $q_{i,e}, i = 1, 2$ denotes the values of the angles at the start and the end of the path in the optimum location.

TABLE VII. Lengths Optimization Results

Links	Lengths
Link 1, l_1	0.1061 m
Link 2, l_2	0.0607 m
Link 3, l_3	0.1061 m
Link 4, l_4	0.1779 m

TABLE VIII. Path Location Optimization Results

Axis	Location of point C (Fig. 1)
X	0.0644 m
Y	-0.1264 m

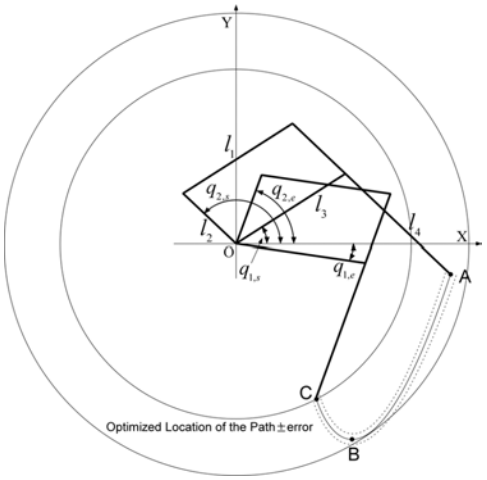

Figure 6. Optimized link lenghts and location of the typical path.

According to the optimization results we have that $l_3 / l_{4-2} = 0.9$, that along the path $1.37 rad \le q_2 - q_1 \le 1.97 rad$ and that at point C, $q_2 - q_1 = 1.37 rad$ and $q_2 = 1.22 rad$. The new mechanism, configured at the end of the optimized path (point C in Fig. 6), is presented in Fig. 7 as CAD drawing. The haptic device is now under construction and we expect to be ready for evaluation in two weeks.

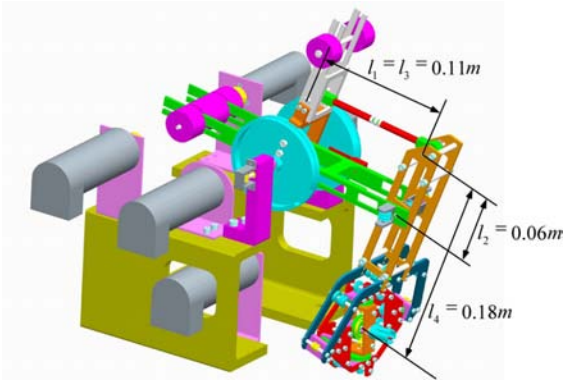

Figure 7. The optimized mechanism in CAD drawing

V. Discussion

As we can see in Fig. 6 the path can be contained between two circles indicating the maximum and minimum distance of endoscope tip from point O. The difference between maximum and minimum distance from point O tends to be minimum, taking into account the various constraints. In other words, the path location that results tends to be as much circular as possible, relative to point O. This is expected because we know that a circular path gives minimum condition number, which is one of our requirements. Other locations, which give better results relative to the condition number, may be obtained from the optimization procedure but these locations contradict to several operational constraints.

The optimization gives a reduction of the link lengths of about 20% relative to the previous mechanism. Furthermore a reduction to the mass matrix diagonal terms of the 5 – bar mechanism of about 40% is calculated.

VI. Conclusions

A design methodology which aims at the minimization of the mass, inertia and joint friction for a low – force five – dof haptic device is presented. The haptic device is optimized along a typical path, rather than at some workspace operating point. The minimized objective functions include mass/ inertia properties and joint friction. The optimization took into account several kinematical and operational constraints that are detailed described. Significant better results are obtained with respect to an existing device.

References

[1] Laguna, M. P., Hatzinger, M., and Rassweiler, J., 2002, "Simulators and endourological training," *Current Opinion in Urology 2002*, vol. 12, pp. 209 – 215.

[2] Chen, E., Marcus, B., 1998, "Force Feedback for Surgical Simulation," in *Proceedings of the IEEE*, 86, pp. 524 – 530.

[3] Salisbury, J. K., Srinivasan, A. M., 1997, "Projects in VR. Phantom – Based Haptic Interaction with Virtual Objects," *IEEE Computer Graphics and Applications*, pp. 6 – 10.

[4] D'Aulignac, D., Balaniuk, R., Laugier, C., 2000, "A Haptic Interface for a Virtual Exam of the Human Thigh," in *Proc. IEEE Int. Conference on Robotics and Automation*, pp. 2452 – 2457.

[5] Atsuko, T., Koichi, H., Toyohisa, K., 1998, "Virtual Cutting with Force Feedback," in *Proceedings of the Virtual Reality Annual International Symposium*, pp. 71 – 75.

[6] Baumann, R., et al., 1997, "The PantoScope: A Spherical Remote – Center – of – Motion Parallel Manipulator for Force Reflection," in *Proc. IEEE Int. Conference on Robotics and Automation*, pp. 718 – 723.

[7] Baur, C., Guzzoni, D., Georg, O., 1998, "Virgy, A Virtual Reality and Force Feedback Based Endoscopy Surgery Simulator," in *Proceedings – Medicine Meets Virtual Reality '98*, (MMVR'98), pp. 110 – 116.

[8] Kühnapfel, U., et al., 1997, "The Karlsruhe Endoscopic Surgery Trainer as an example for Virtual Reality in Medical Education," in *Minimally Invasive Therapy and Allied Technologies (MITAT)*, pp. 122-125, Blackwell Science Ltd.

[9] Vlachos, K., Papadopoulos, E., and Mitropoulos, D. N., 2003, "Design and implementation of a haptic device for training in urological operations," *IEEE Transactions on Robotics and Automation*, vol. 19, no. 5, October 2003, pp. 801 – 809.

[10] Khatib, O. and Bowling, A., 1996, "Optimization of the inertial and acceleration characteristics of manipulators," *Proc. IEEE International Conference on Robotics and Automation (ICRA'96)*, Minneapolis, Minnesota, April 1996, vol. 4, pp. 2883-2889.

[11] Stocco, L., Salcudean, S. E., and Sassani, F., 1999, "Fast constrained global optimization of robot parameters," *Robotica*, Vol.16, pp.595-605.

[12] Stocco, L. J., Salcudean, S. E., and Sassani, F., 2001, "Optimal kinematic design of a haptic pen," *IEEE/ASME Transactions on Mechatronics*, vol. 6, no. 3.

[13] Hayward, V., Choksi, J., Lanvin, G., and Ramstein, C., 1994, "Design and multi–objective optimization of a linkage for a haptic interface," *Advances in Robot Kinematics and Computationed Geometry*, A. J. Lenarcic and B. B. Ravani (eds.), Kluwer Academic Publishers, pp. 359 – 368.

[14] Kurtz, R., Hayward, V., 1992, "Multiple–goal kinematic optimization of a parallel spherical mechanism with actuator redundancy," *IEEE Transactions on Robotics and Automation*, vol. 8, no. 5, pp. 644 – 651.

[15] Brayton, R.K., S.W. Director, G.D. Hachtel, and L.Vidigal, "A New Algorithm for Statistical Circuit Design Based on Quasi-Newton Methods and Function Splitting," *IEEE Transactions on Circuits and Systems*, Vol. CAS-26, pp. 784-794, Sept. 1979.